Thermochimica Acta, 216 (1993) 1–14
Elsevier Science Publishers B.V., Amsterdam

An optimised equilibrium phase diagram and solution thermodynamics of arsenic–lead alloys

Harri Rannikko [1], Salla Sundström [2] and Pekka Taskinen [3,*]
Helsinki University of Technology, Faculty of Process Engineering and Material Science, Laboratory of Materials Processing and Powder Metallurgy, SF-02150 Espoo (Finland)

(Received 26 June 1992)

Abstract

The thermodynamic properties of solid and liquid arsenic–lead alloys have been critically analysed using the available literature sources. The excess Gibbs energies for the alloy phases were modelled by Redlich–Kister polynomials and the simultaneous least-squares analysis of the experimental data was carried out by using the LUKAS program. The following integral excess Gibbs energy functions were estimated for the liquid alloy and the lead fcc solid solution (J mol^{-1})

$$ {}^{\mathrm{Ex}}G_{\mathrm{liq}} = x_{\mathrm{As}}x_{\mathrm{Pb}}[1835.46 - 6.20869T + (-1857.52 - 3.50418T)(x_{\mathrm{As}} - x_{\mathrm{Pb}})] $$

$$ {}^{\mathrm{Ex}}G_{\mathrm{fcc}} = x_{\mathrm{As}}x_{\mathrm{Pb}}[14076.6] $$

The eutectic point was calculated as being at ${}^{\mathrm{e}}T = 565.64$ K with ${}^{\mathrm{fcc}}x_{\mathrm{As}} = 0.00150$, ${}^{\mathrm{e}}x_{\mathrm{As}} = 0.0664$ and ${}^{\mathrm{rho}}x_{\mathrm{As}} = 1.0000$.

The limiting activity coefficients of the components at infinite dilution in liquid lead and arsenic, respectively, calculated from the optimised model parameters were

$$ \ln {}^{\circ}f_{[\mathrm{As}]} = -0.325 + 444.17/T\ (\mathrm{K}) $$

$$ \ln {}^{\circ}f_{[\mathrm{Pb}]} = -1.168 - 2.65/T\ (\mathrm{K}) $$

INTRODUCTION

The mixing thermodynamics and phase diagram of the binary system As–Pb have been re-evaluated using a computerised optimisation procedure [1]. This work updates a preliminary study by Sundström and Taskinen [2], including the most recent references and the lattice stabilities in the SGTE form.

A recent version of the LUKAS program for microcomputers (ver.

---

* Corresponding author.

[1] Present address: Outokumpu Research Oy, P.O. Box 60, SF-28101 Pori, Finland.

[2] Present address: Rautaruukki, Oy, Research Centre, SF-92101 Raahe, Finland.

[3] Present address: Outokumpu Research Oy, P.O. Box 60, SF-28101, Pori, Finland.

91-3/1991) [3] has been used in this work. The optimisation and phase diagram calculation software was developed by H.-L. Lukas at the Max-Planck-Institut für Metallforschung (PML) in Stuttgart [1]. The program uses a least-squares method for fitting simultaneously the thermodynamic mixing functions and the phase diagram from different types of experimental observations, such as calorimetric, e.m.f. or vapour pressure data, and tie lines from phase diagram measurements. The aim of the least-squares analysis is a consistent set of thermodynamic model parameters describing the entire system for calculation of the phase diagram and the thermodynamic functions of all the phases [1].

THERMODYNAMIC MODELS

The SGTE format [4] for the temperature dependency of the Gibbs energies of the pure species was used, with

$$
\begin{aligned}
{}^{\circ}G_i - H_i^{\mathrm{SER}} &= A + BT + CT\ln T + DT^2 + E/T + FT^3 \\
&\quad + GT^4 + HT^7 + IT^{-9}
\end{aligned}
\tag{1}
$$

where A to I are temperature independent coefficients and H_i^{SER} is the enthalpy of the most stable phase of species i at 298.15 K.

The molar Gibbs energies for the alloys were described in the following form, assuming substitutional structures for the phases.

$$
G = {}^{\mathrm{ref}}G + {}^{\mathrm{id}}G + {}^{\mathrm{Ex}}G \tag{2}
$$

where G is the integral Gibbs energy of the phase, ${}^{\mathrm{ref}}G = \sum x_i {}^{\circ}G_i$ is the reference surface of the Gibbs energy, $\mathrm{id}_G = RT\sum x_i \ln x_i$ is the ideal mixing term, and $\mathrm{Ex}_G = \sum x_i {}^{\mathrm{Ex}}G_i$ is the excess term of the Gibbs energy.

The integral excess Gibbs energy for a substitutional, binary alloy phase can be written by Redlich–Kister polynomials [5] as follows

$$
{}^{\mathrm{Ex}}G = x_{\mathrm{As}} x_{\mathrm{Pb}} \sum A_i (x_{\mathrm{As}} - x_{\mathrm{Pb}})^i \tag{3}
$$

where A_i are adjustable coefficients to be calculated in the least-squares optimisation. The general form for the temperature dependency of the coefficients A_i is given by eqn. (1).

The limiting activity coefficients of the components As and Pb at infinite dilution were calculated by using the general formulae for partial Gibbs excess energies given recently by Hillert [6]

$$
{}^{\mathrm{Ex}}G_{\mathrm{As}} = RT\ln f_{\mathrm{As}} = x_{\mathrm{As}}^2[A_0 + \sum A_i (x_{\mathrm{As}} - x_{\mathrm{Pb}})^{i-1}[(2i+1)x_{\mathrm{As}} - x_{\mathrm{Pb}}]] \tag{4}
$$

$$
{}^{\mathrm{Ex}}G_{\mathrm{Pb}} = RT\ln f_{\mathrm{pb}} = x_{\mathrm{Pb}}^2[A_0 + \sum A_i (x_{\mathrm{As}} - x_{\mathrm{Pb}})^{i-1}[x_{\mathrm{As}} - (2i+1)x_{\mathrm{Pb}}]] \tag{5}
$$

GENERAL DESCRIPTION OF THE SYSTEM As–Pb

Pure lead metals at 600.65 K [7] and solidifies in an fcc lattice [8]. The crystal structure of pure arsenic is rhombohedral; at 1 atm it sublimates at 887 K forming a complex atmosphere of arsenic polymers, $As_n(g)$ with $n = 1–4$. The melting point of arsenic is 1090 K at 35.8 atm [8, 9].

The binary phase diagram is of eutectic type. No stable intermetallic compounds have been found and there is a complete miscibility in the liquid state [10]. The maximum solubility of arsenic in solid lead is very small, with $^{fcc}x_{As} = 0.14$ at.% [10] attained at the eutectic temperature.

LITERATURE DATA

The formulation of the alloy system has been studied by several authors. Hansen and Anderko [10] have compiled the phase diagram studies up to 1958. The reviews by Schlesinger and Lynch [11] and Gokcen [12] critically compiled the thermodynamic observations on molten and solid As–Pb alloys.

Pure elements As and Pb

The Gibbs energies for pure elements with reference to SER (stable element reference) at 298.15 K and 1 bar were taken from the recent SGTE assessment by Dinsdale [4]. The values of the coefficients A to I in eqn. (1) used in the calculations are shown in Table 1.

The alloy phases

Among the first studies on the constitution of the As–Pb system were the investigations of Heycock and Neville (1982) [13] and Friedrich (1906) [14]. Also, Heike [15] determined the liquidus line for alloys with as high as 82.3 at.% arsenic, which is the highest arsenic concentration in As–Pb melts studied experimentally so far. Hansen and Anderko [10] collected the phase diagram investigations of the system and published a complete phase diagram. Hutchison and Peretti [16] redetermined the high-lead end of the system with the aid of the cooling curves. E.m.f. techniques have also been used for determining liquidus temperatures [17, 18]. Hutchison and Peretti have also critically evaluated some earlier published experimental values [15, 19, 20].

The solubility of arsenic in solid lead has been studied by Nishikara [21] and more recently by Tsumuraya [22]. Nishikara obtained his results from hardness–composition curves and Tsumuraya used electrical resistivity measurements. Bauer and Tonn [19] have also studied the solid solubility as

TABLE 1

The lattice stabilities of arsenic and lead, $^{\circ}G_i - H_i^{\mathrm{SER}}$, and the Gibbs energy differences of the pure metastable species used in the calculations [4] (J mol^{-1})

As (rho)
298.15–1090 K:
$-7270.447 + 122.211069T - 23.3144T \ln T - 2.71613 \times 10^{-3}T^2 + 1.16 \times 10^4/T$
1090–1200 K:
$-10454.913 + 163.457433T - 29.216037T^2$

Pb (liq)
298.15–600.65 K:
$-2977.928 + 93.964931T - 24.5242231T \ln T - 3.65895 \times 10^{-3}T^2 - 2.4395 \times 10^{-7}T^3$
$- 6.0144 \times 10^{-9}T^7$
600.65–1200 K:
$-5678.003 + 146.191568T - 32.4913959T \ln T + 1.54613 \times 10^{-3}T^2$
1200–5000 K:
$9010.708 + 45.087458T - 18.9640637T \ln T - 2.882943 \times 10^{-3}T^2 - 2.696755 \times 10^6/T$
$+ 9.8144 \times 10^{-8}T^3$

Pb (fcc)
298.15–600.65 K:
$-7650.085 + 101.715188T - 24.5242231T \ln T - 3.65895 \times 10^{-3}T^2 - 2.4395 \times 10^{-7}T^3$
600.65–1200 K:
$-10531.115 + 154.258155T - 32.4913959T \ln T + 1.54613 \times 10^{-3}T^2 + 8.05644 \times 10^{25}T^{-9}$
1200–5000 K:
$4157.596 + 53.154045T - 18.9640637T \ln T - 2.882943 \times 10^{-3}T^2 - 2.696755 \times 10^6/T$
$+ 9.8144 \times 10^{-8}T^3 + 8.05644 \times 10^{25}T^{-9}$

$G^{\circ}(\mathrm{As, liq}) - G^{\circ}(\mathrm{As, rho}) = 24442.9 - 22.42468T$

$G^{\circ}(\mathrm{As, fcc}) - G^{\circ}(\mathrm{As, rho}) = 24874.0 - 14.740T$

well as molten As–Pb alloys in the compositional region 0–28 at.% arsenic. Unfortunately, they published only a few solubility values in numerical form.

The solubility of lead in solid arsenic is mentioned on only a few occasions. According to Heike [15], lead is soluble in solid arsenic to only the very smallest extent. Schlesinger and Lynch [11] believe that there is no measurable solid solubility. No experimental data are available, and the solubility was neglected in the present calculations assuming As(rho) as a pure, unary phase.

E.m.f. methods [17, 23, 24] as well as vapour pressure and isopiestic techniques [25–27] have been used for determining the thermodynamic properties of the As–Pb system. The most recent e.m.f. data using lead concentration cells with molten electrolytes reported by Onderka and

TABLE 2

Summary of thermodynamic and phase diagram studies on As–Pb alloys

Phase diagram		Thermodynamic data				Errors			
Equil.	Dynamic	H	μ_{Pb}	μ_{As}	Method	Δv [a]	ΔT	Δx	Ref.
	x				TA		4	0.02	13
	x				TA		5	0.03	14
	x				TA		5	0.04	15
	x				TA		1	0.005	16
			x		E.m.f.	10%	3.5	0.01	17
x					E.m.f.		5.5	0.01	17
			x		E.m.f.	10%	2	0.01	18
x					E.m.f.		3	0.01	18
	x				TA		2.5	0.01	19
	x				TA		2	0.05	20
x					Hardness		3	0.03	21
x					Electric res.		2	0.01	22
			x		E.m.f.	5–10%	2.5	0.015	23
			x		E.m.f.	20%	2	0.01	24
				x	Vapour pr.	10%	2	0.01	25
		x			Calorim.	7%	5	0.01	26
				x	Vapour pr.	20%	4	0.01	26
x					Isopiestic	20%	4	0.04	27
				x	Isopiestic	10%	2	0.015	27
		x			Calorim.	–	–	–	28 [b]

[a] Value: ΔH, μ_{Pb}, μ_{As}. [b] Not used in calculations.

Wypartowicz [18] were also included in the optimisation. In their review, Schlesinger and Lynch [11] found a good agreement between independent data at low temperatures (776–855 K). At higher temperatures the agreement decreased, depending on the experimental method used.

Direct measurements on the enthalpies of mixing were published by Predel and Emam [26] and Rtskhiladze et al. [28] only. Because of the significant scatter in the results of Rtskhiladze et al., their values were omitted from the final calculations. The mixing enthalpies derived from chemical potentials in e.m.f. measurements [23] were omitted.

All the experimental studies avalilable in the literature and those used in the final least-squares calculations are listed in Table 2. In addition to the type of data and the method applied, the experimental errors used in the final optimisation for each measured thermodynamic value, for the experimental temperature and for the composition are also given in the table.

RESULTS AND DISCUSSION

The optimisation of the model parameters A_i in eqn. (3) was carried out on two phases. The lead solid solution and the liquid phase were treated as alloys and solid arsenic as a pure unary phase.

TABLE 3

The optimised Redlich–Kister coefficients, eqn. (3), for the alloy phases, $A_i = A_{i0} + A_{i1}T(\mathrm{K})$ ($\mathrm{J\,mol^{-1}}$)

Phase\Coefficient	A_{i0}	A_{i1}
Liquid		
A_0	1835.46	−6.20869
A_1	−1857.52	−3.50418
Pb (fcc)		
A_0	14076.65	–

In the course of the optimisation it was found that no temperature dependency was needed for the parameters of the fcc alloy. The first-order concentration coefficient with the enthalpy and entropy terms was required for the liquid phase. This implies a value $\Delta c_p = 0$ for the formation of the molten alloy. The coefficients for the excess Gibbs energies obtained in the least-squares optimisation procedure, giving a full thermodynamic description to the alloy phases of the system, are collected in Table 3.

The calculated phase diagram

The phase diagram calculated in this work obtained using the optimised model parameters in Table 3 is shown in Fig. 1. The calculated invariant points are also reproduced in the graph. Figure 2 compares the calculated line with the points obtained experimentally on the liquidus. The lead-rich liquidus is well known and the calculated line is in good agreement with the observed data, except for a single point derived by Suleimanov et al. [17]. The studies by Hutchinson and Peretti [16] and Onderka and Wypartowicz [18] reliably reproduce the arsenic-rich liquidus up to 55 at.% As. Itagaki et al. [27], extrapolating the solid arsenic saturation from homogeneous alloys, seem to derive too low arsenic concentrations on the liquidus. This is also the case for most of the older data obtained by thermal analysis on the liquidus temperature.

The eutectic point was calculated to be located at ${}^{e}T = 565.64\,\mathrm{K}$ (292.5°C) with an arsenic concentration in the melt of ${}^{e}x_{\mathrm{As}} = 6.64$ at.%. The experimental investigations on the eutectic point are collected in Table 4 which thus compares the primary data in the literature. The calculated compositions of the eutectic point and the fcc solid solution are in good agreement with those estimated by Gokcen [12]. The eutectic temperature is 1.5°C higher than that selected in his assessment.

The optimised eutectic point is in good agreement with the experimental results of Hutchison and Peretti [16]. Hajicek [20] found a relation between

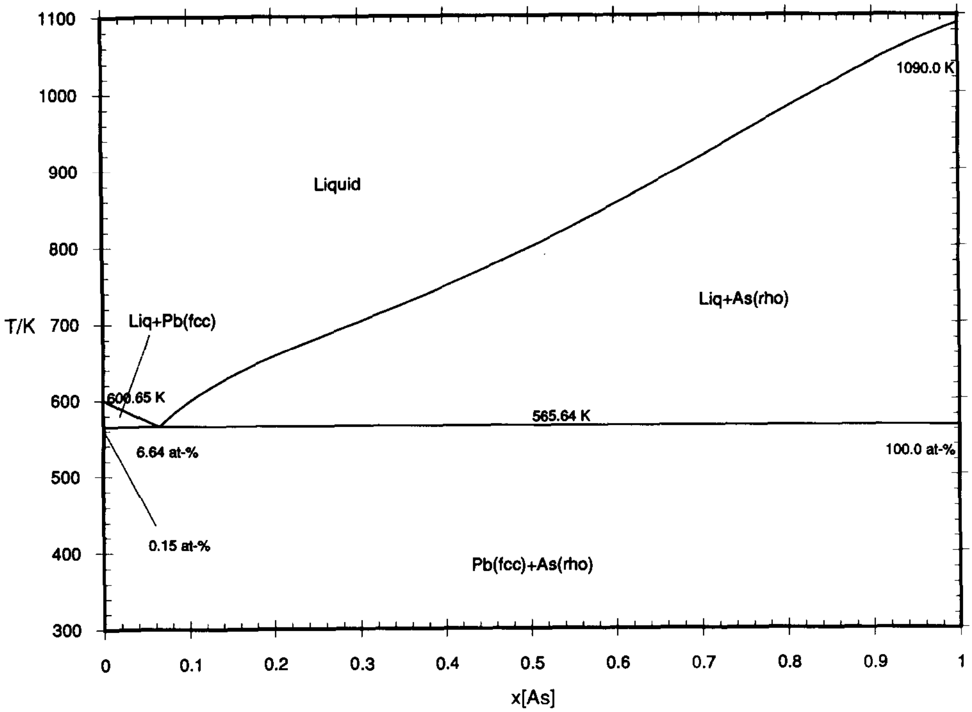

Fig. 1. The optimised As–Pb phase diagram calculated at 300–1100 K omitting the gas phase.

the composition and the melting temperature of the eutectic and the melting temperatures of individual components in simple binary alloys [20]. Calculating the eutectic point in this way he estimated for the As–Pb system, $^{e}t = 292^{\circ}\mathrm{C}$ and $^{e}x_{\mathrm{As}} = 11.15$ at.%. For the eutectic temperature, this result is in good agreement with other reports, but the arsenic content of the eutectic is much higher. The low eutectic temperature obtained using thermal analysis techniques by Heike [15] and Bauer and Tonn [19] are evidently caused by supercooling [16]. The effect is seen in Fig. 2 where the values of Heike are systematically below the calculated liquidus line. This is also supported by the good accordance of the liquidus data of Onderka and Wypartowicz [18] obtained by e.m.f. techniques. Hansen and Anderko [10] have incorrectly referred the arsenic content at the eutectic point reported by Heike [15], giving $^{e}x_{\mathrm{As}} = 7.4 \pm 0.5$ at.% at $^{e}t = 288^{\circ}\mathrm{C}$.

The calculated fcc solid solution is shown in Fig. 3 together with the experimental points obtained by different methods [21, 22]. The maximum solubility of arsenic in lead was calculated to be 0.150 at.% As at the eutectic temperature $^{e}t = 292.5^{\circ}\mathrm{C}$. Despite the small concentrations of arsenic, the experimental results are in excellent agreement and they are well reproduced by the calculated curve down to 408 K (135°C). Bauer and

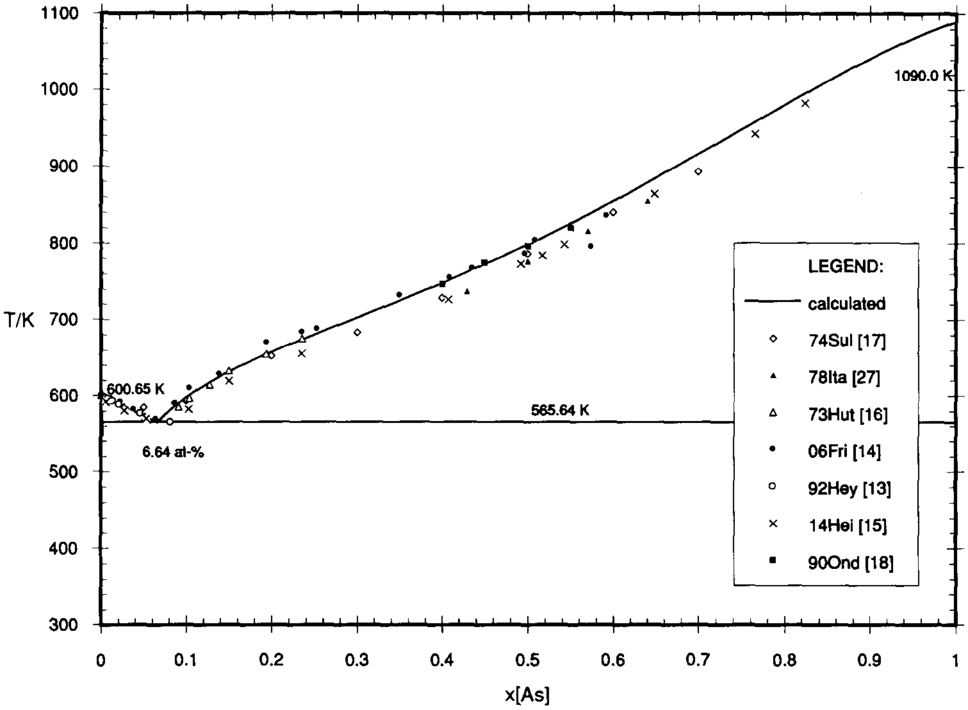

Fig. 2. A comparison of the optimised As–Pb phase diagram with the experimental liquidus values: Heycock and Neville [13], Friedrich [14], Heike [15], Hutchison and Peretti [16], Suleimanov et al. [17], Onderka and Wypartowicz [18] and Itagaki et al. [27].

TABLE 4

Summary of the eutectic data for the As–Pb system

Investigator	Ref.	^{e}t (°C)	$^{fcc}x_{As}$ (at.%)	$^{e}x_{As}$ (at.%)
Experimental				
Friedrich (1906)	14	292.0		6.6–7.9
Heike (1914)	15	288.0		8.25
Hutchison (1973)	16	291.0		6.62 ± 0.25
Bauer (1935)	19	290.0	0.14	6.88
Hajicek (1948)	20	292.0		11.15
Assessed values				
Hansen and Anderko	10	288		7.4
Gokcen	12	291.0	0.13	6.85
This work		292.5	0.150	6.64

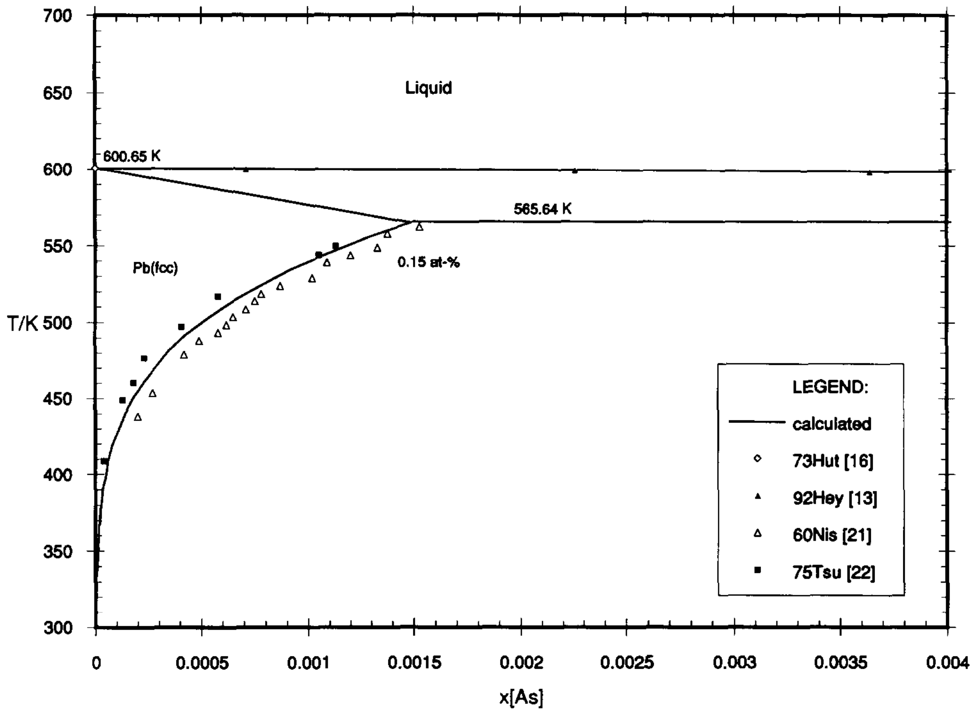

Fig. 3. Solubility of arsenic in solid lead: the optimised fcc solid solution area with the experimental data of Heycock and Neville [13], Nishikara [21] and Tsumuraya [22].

Tonn [19] reported the solubility of arsenic in solid lead to be 0.14 at.% at 290°C. They also estimated the solubility at room temperature to be less than 0.3 at.% As. In this work, the solid solubility at room temperature calculated using the optimised model parameters is much smaller than their upper limit, less than 0.001 at.% [As].

The thermodynamic properties of the liquid phase

The assessed activity curves for arsenic and lead at 673 K and 1073 K in the molten alloy are shown in Fig. 4. Arsenic shows a negative deviation from the Raoultian solution at concentrations above 10 at.% As. The activity curve of lead changes its positive deviation from the Raoultian solution to a negative one at an arsenic concentration of about 60 at.% As. Selected primary data on the chemical potential of arsenic in the molten alloy are reproduced in Fig. 5 and compared with the calculated values at 673, 873 and 1073 K.

The activity coefficients of the components at infinite dilution in liquid lead and arsenic, respectively, were calculated from the assessed model parameters in Table 3 by using eqns. (4) and (5): $\ln {}^{\circ}f_{[\mathrm{As}]} = -0.325 + 444.17/T(\mathrm{K})$ and $\ln {}^{\circ}f_{[\mathrm{Pb}]} = -1.168 - 2.65/T(\mathrm{K})$.

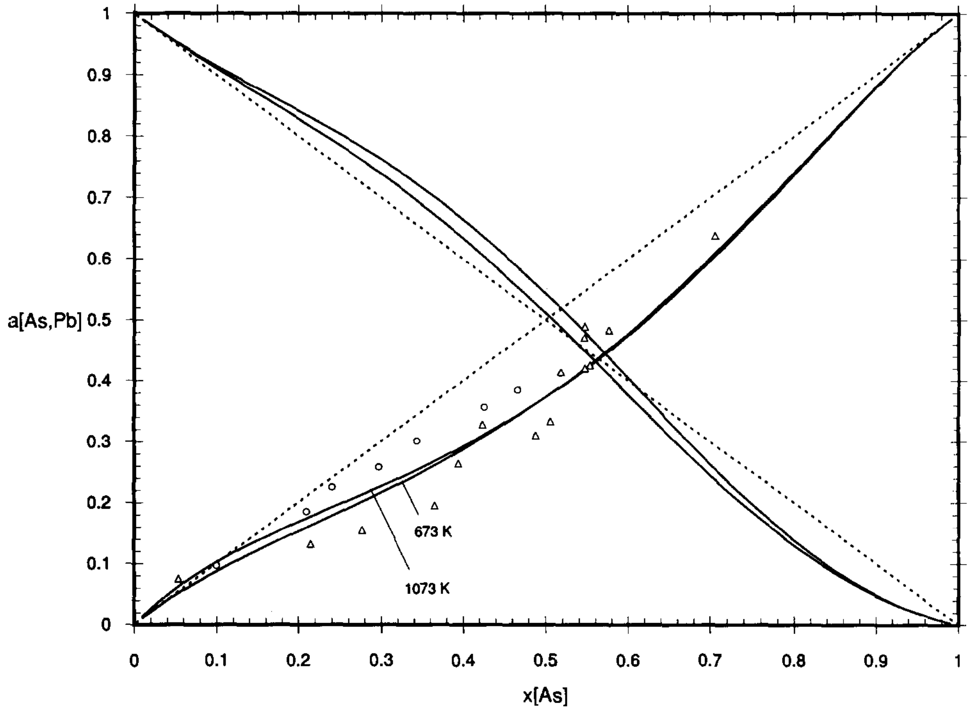

Fig. 4. The assessed activities of arsenic and lead at 673 and 1073 K in liquid As–Pb alloys, omitting the solubility limits of arsenic, with: △, experimental data reported by Predel and Emam [26] at 913 K; and ○, by Itagaki et al. [27] at 855 K; the standard states are As(l) and Pb(l).

The activity coefficients of arsenic obtained at infinite dilution in liquid lead are also shown in Fig. 6 as a function of the inverse of the absolute temperature. A comparison is made in the figure with the experimental values given by Itagaki et al. [27] and by Onderka and Wypartowicz [18].

The consistency of the assessed parameters and the recent experimental data of Onderka and Wypartowicz [18] on molten As–Pb alloys was checked by comparing the e.m.f. values of a lead concentration cell:

(−)Pb/KCl–LiCl–$PbCl_2$/Pb–As(+)

without those calculated from the optimised model parameters. The discreet e.m.f. values used in the optimisation, estimated from the authors' T–E plots, and the calculated curves obtained using the optimised model parameters determined in this work, are shown in Fig. 7. The agreement is very good at low arsenic concentrations, below 40–45 at.% As, and even in arsenic-rich alloys the deviation is only 1–2 mV.

The calculated integral enthalpy of mixing of molten As–Pb alloys is shown in Fig. 8 with the experimental values reported by Predel and Emam [26]. Due to the type of the mixing functions selected by eqn. (1), with only two terms in each excess parameter, the enthalpy of mixing of molten

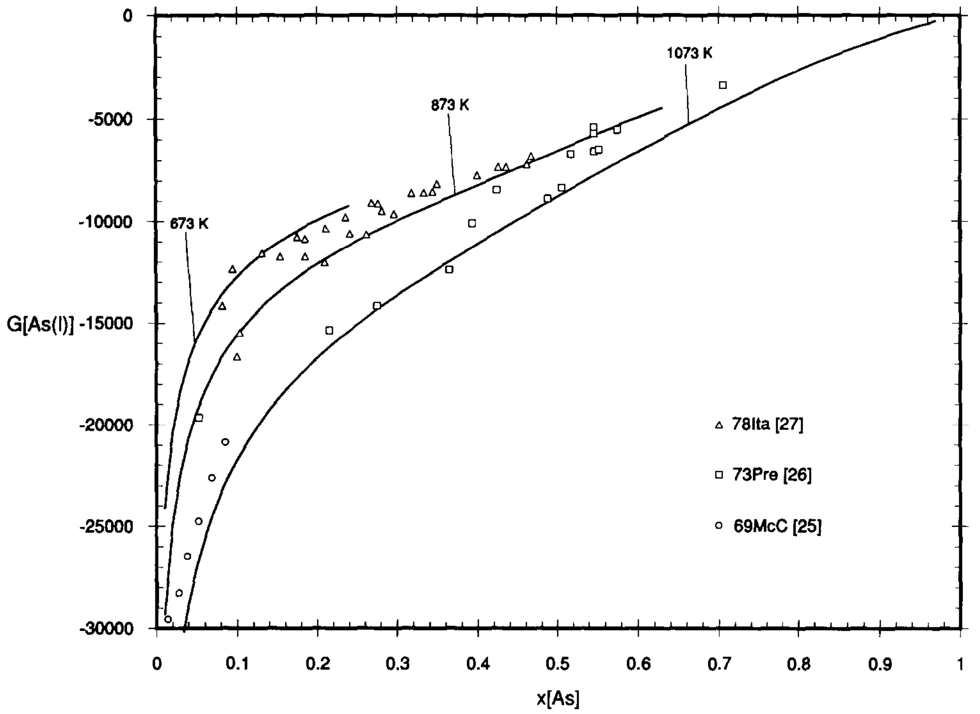

Fig. 5. The chemical potential of arsenic calculated at 673, 873 and 1073 K, together with the experimental values used in the optimisation; the molten alloy is saturated with As(rho) at 24, 63 and 97 at.% As, respectively; the standard state is As(l).

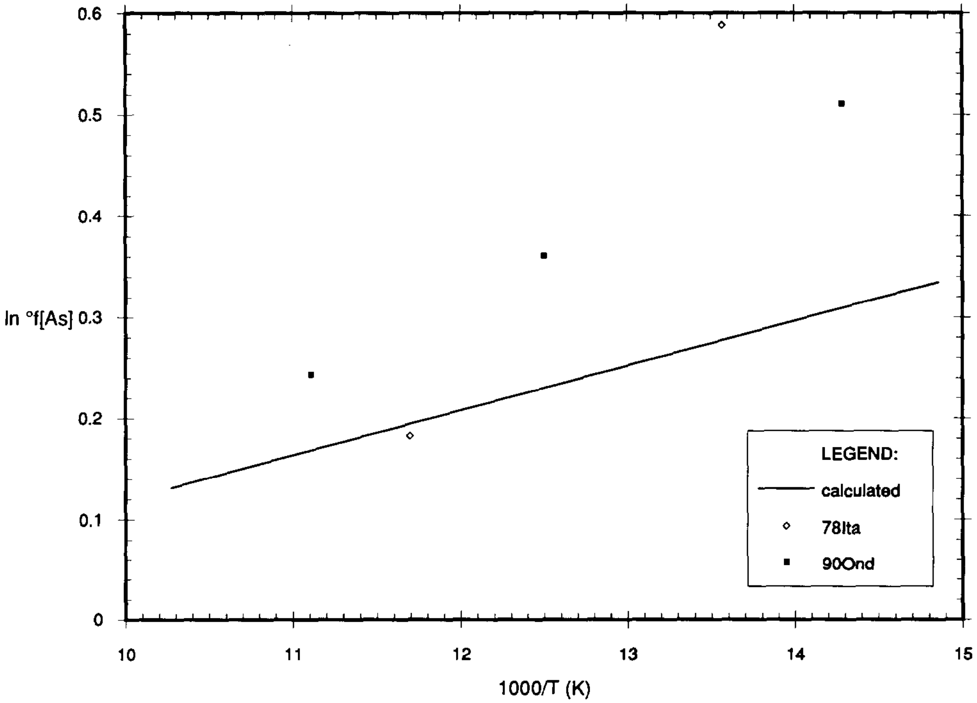

Fig. 6. The logarithmic activity coefficient of arsenic at infinite dilution in molten lead as a function of the inverse absolute temperature.

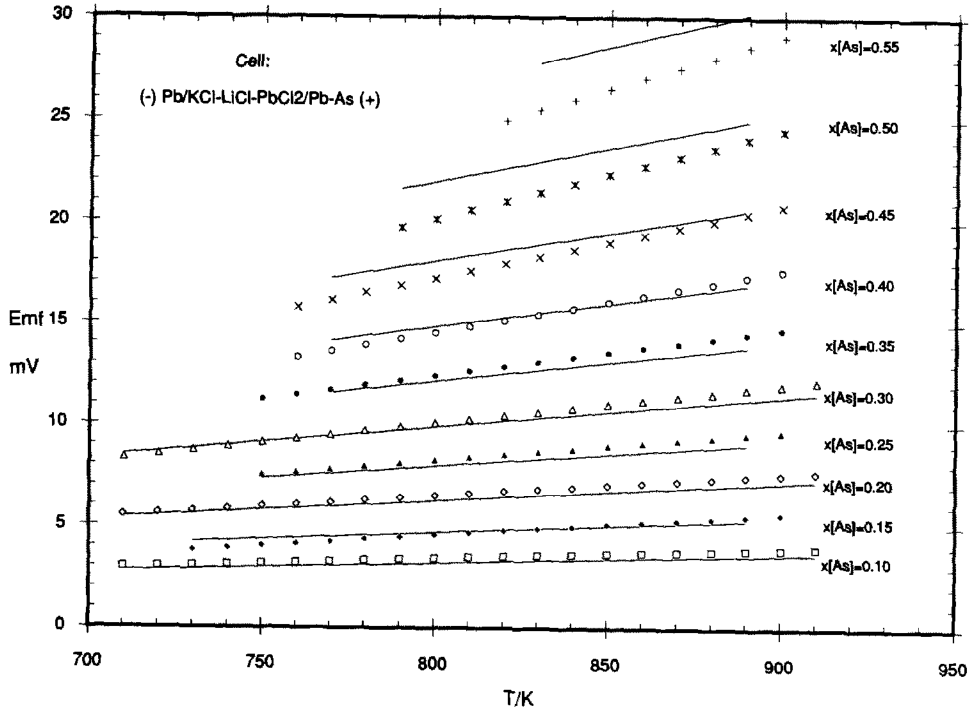

Fig. 7. A comparison of the calculated (——) and experimental [18] e.m.f. values of lead concentration cells: (−)Pb/KCl,LiCl,$PbCl_2$/[Pb,As](+).

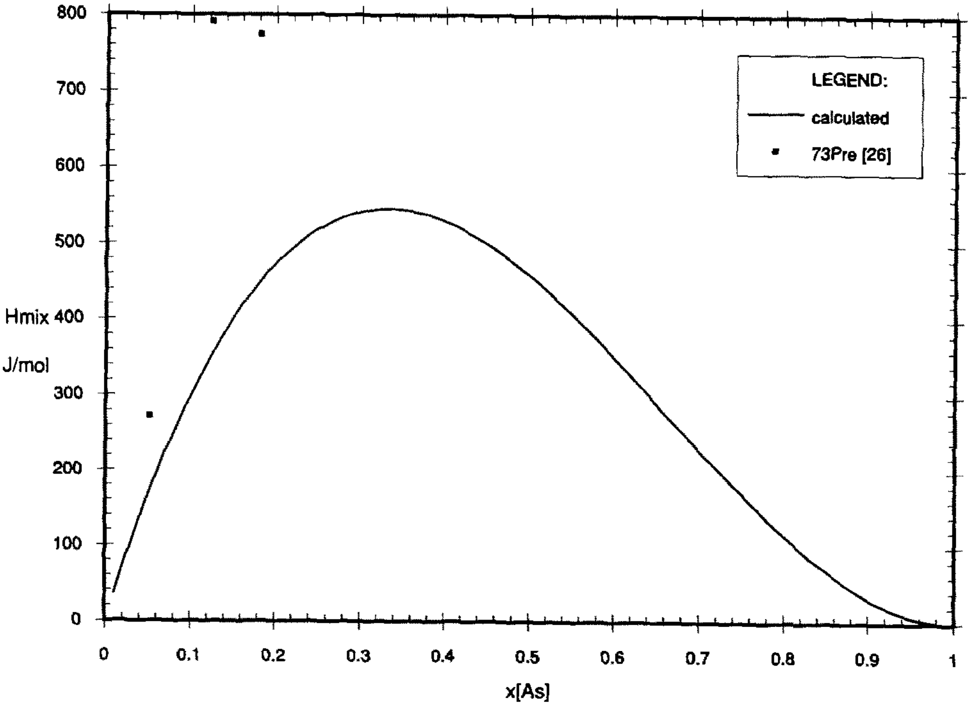

Fig. 8. The optimised, temperature-independent integral enthalpy of mixing of liquid As–Pb alloys with the experimental values by Predel and Emam [26] at 520°C; the standard states are As(l) and Pb(l).

As–Pb alloys is independent of temperature. According to Predel and Emam, its positive values can be essentially attributed to a misfit in the atomic structure of the As–Pb alloys, due to differences in the atomic volume of the components. Experimental data are too scarce, conflicting [26, 28] and scattered for any conclusions to be made on the mixing enthalpy.

On the basis of the present assessment, future experimental work on the As–Pb binary system should be directed to arsenic-rich alloys and to accurate measurements of mixing enthalpies in molten alloys. The absence of this information clearly lowers the accuracy of the present optimised model data in alloys richer in arsenic than about 50–60 at.%.

ACKNOWLEDGEMENTS

The authors are indebted to Professor Kaj Lilius of HUT for the provision of the research facilities needed in this work. Special thanks are due to Dr. H.-L. Lukas of the Max-Planck-Institut für Metallforschung in Stuttgart for the availability of updated versions of the optimisation program.

REFERENCES

1 H.-L. Lukas, E.-Th. Henig and B. Zimmermann, Calphad, 3 (1977) 225.
2 S. Sundström and P. Taskinen, The Optimised Equilibrium Phase Diagram and Solution Thermodynamics of the As–Pb alloys, Helsinki University of Technology, Report No. TKK-V-B50, Otaniemi, Finland, 1989.
3 H.-L. Lukas, S. Fries, U. Kattner and J. Weiss, Manual of the Computer Programs BINGSS, BINFKT, TERGSS and TERFKT, Version 91-3, Freiburg, FRG, 1991.
4 A.T. Dinsdale, SGTE Data for Pure Elements, National Physical Laboratory (UK), NPL Report No. DMA(A) 195, Sept. 1989; Calphad, 15 (1991) 317.
5 A. Pelton and C. Bale, Metall. Trans. A, 17A (1986) 1057.
6 M. Hillert, Thermochim. Acta, 129 (1988) 7.
7 Melting Points of the Elements, Bull. Alloy Phase Diagrams, 2 (1981) 146.
8 H. King, Bull. Alloy Phase Diagrams, 2 (1981) 402.
9 N.A. Gokcen, Bull. Alloy Phase Diagrams, 10 (1989) 11.
10 M. Hansen and K. Anderko, Constitution of Binary Alloys, McGraw-Hill, New York, 1958.
11 M.E. Schlesinger and D.C. Lynch, Metall. Trans. B, 17B (1986) 235.
12 N.A. Gokcen, Bull. Alloy Phase Diagrams, 11 (1990) 120.
13 C.T. Heycock and F.H. Neville, J. Chem. Soc., 61 (1892) 888.
14 W. Friedrich, Metallurgie, 3 (1906) 41.
15 W. Heike, Intern. Z. Metallogr., 6 (1914) 183.
16 S. Hutchison and E.A. Peretti, J. Less-Comm. Met., 30 (1973) 306.
17 D. Suleimanov, A. Mamedov and A. Kuliev, Izvt. Vyssh. Uchebn. Zaved., Khim. Khim. Tekhnol., 17 (1974) 3, 365.
18 B. Onderka and J. Wypartowicz, Z. Metallkde., 81 (1990) 345.
19 O. Bauer and W. Tonn, Z. Metallkde., 27 (1935) 183.
20 O. Hajicek, Hutn. Listy, 3 (1948) 265.

21 S. Nishikara, Tokyo University, Production Technique Institute Report 9, 1960, 92 pp.
22 K. Tsumuraya, Meiji Daigaku Kagaku Gijutsu Kenkyusho Kiyo, 14 (1975) 1.
23 E. Zaleska, Rocz. Chem., Ann. Soc. Chim. Polon., 48 (1974) 195.
24 J. Moriyama, Z. Kozuka and H. Miura, Suiyou Kaishi, 15 (1964) 191.
25 R.J. McClincy and A.H. Larsen, Trans. AIME, 245 (1969) 647.
26 B. Predel and A. Emam, Z. Metallkde., 64 (1973) 647.
27 K. Itagaki, T. Shimizu and M. Hino, Bull. Research Institute of Mineral Dressing and Metallurgy, Tohoku University (Sendai), 34 (1978) 45.
28 V.G. Rtskhiladze, L.A. Chkhikvadze and E.T. Tkhilava, Bull. Acad. Sci. Georgian SSR, 109 (1983) 105.